THE BELL SYSTEM
TECHNICAL JOURNAL

DEVOTED TO THE SCIENTIFIC AND ENGINEERING
ASPECTS OF ELECTRICAL COMMUNICATION

Volume 51 February 1972 Number 2

Multipath Propagation at 4, 6, and 11 GHz

By W. T. BARNETT

(Manuscript received August 24, 1971)

Signals at 4, 6, and 11 GHz, transmitted over a 28.5-mile radio relay path in Ohio, were continuously monitored during the late summer of 1966. Previous publications have reported on the observed 4- and 6-GHz multipath fading statistics, and on the improvements available with space or frequency diversity. This paper presents data for the 11-GHz transmission, and, in combination with the earlier results, establishes an empirical frequency dependence for the amplitude statistics.

A general treatment of the relationships between the factors underlying multipath propagation is intractable. However, based on the results in this and other papers, a general relationship is given for the probability of deep multipath fading which is linear in frequency, cubic in path length, and varies with meteorological-geographical factors.

Temporal aspects of the Ohio data were also investigated at all frequencies, utilizing both a 1-hour and a 1-day clock time interval. It was found that the multipath fade time statistic can be described by a single parameter for either interval. A subset of the multipath fading hours was also analyzed using a 1-minute clock interval, with the result that the difference between the minute median fade and the hourly median fade is frequency independent, and normally distributed with a standard deviation of 5.5 dB.

I. INTRODUCTION

Although it is a relatively rare phenomenon, multipath propagation constitutes a fundamental limitation to the performance of microwave

radio systems. During a period of multipath propagation, the narrowband output from a single receiving antenna can be reduced to equipment noise levels for seconds at a time. Corrective measures such as frequency diversity or space diversity then must be introduced to provide satisfactory commercial operation.[1-3] Propagation data required for economical system design and detailed performance estimates were not available prior to 1966. To fill this need an extensive experimental program was undertaken on a typical radio relay path in Ohio. Previous studies[1,2,4] have reported on the amplitude statistics obtaining during multipath propagation at 4 and 6 GHz, both with and without frequency or space diversity. Data were also obtained for a single frequency in the 11-GHz band. The multipath fading data for this signal have now been analyzed and statistics for the total time faded (P), the number of fades (N), their average duration ($\bar{t}$), and the fade duration distribution are presented in Section IV as functions of fade depth.

Multipath propagation is by its very nature dependent upon the operating microwave frequency; the variation of the fading characteristics with frequency has been considered by many investigators[5,6] with controversial results.* This is not surprising considering the time-variant, nonstationary behavior of the phenomena. However, the data obtained in Ohio were extensive enough to give statistical stability which, with the 11:6:4 frequency sampling, allows a meaningful comparison in Section V of P, N, and $\bar{t}$ as functions of frequency.

It is clear that a great deal is known about one path in Ohio. Generalization of these results to other paths requires an underlying theory. The experimental data show that P, N, and $\bar{t}$ can be quite closely represented by simple, one-term algebraic functions of fade depth. This agrees with predictions by S. H. Lin[7] based on analysis of a simple and plausible analytic model for multipath fading. It is therefore reasonable to assume that the variation of P, N, and $\bar{t}$ with fade depth for all paths subject to multipath fading will have the same functional dependence as did the Ohio path. A general formulation which includes the most important path parameters is proposed in Section VI for the coefficient in the equation relating the total time faded and the fade depth during the so-called worst fading month. This estimate provides necessary information for microwave radio system design in the continental U.S.A.

The intensity of multipath fading varies greatly, even during the normally active summer months; during some days there will be exten-

* Reference 5 gives many references on multipath fading investigations.

sive multipath fading, while on others there will be none. Statistics for time bases shorter than a month—or the entire 68-day period for the test reported here—are also of interest. The time faded characteristic was studied for the 4-, 6-, and 11-GHz signals on both a daily (24-hour) and an hourly basis. Section VII concludes with a study of minute-by-minute variations within an hour for a subset of the multipath fading hours.

All the experimental results mentioned in the preceding paragraphs were obtained from a data base comprising all the time intervals with deep multipath fading.[2] In sum, these intervals were about 15 percent of the total measurement time. The P, N, and $\bar{t}$ statistics for the remaining 85 percent of the time are given in Section VIII for typical 4- and 6-GHz signals. The 11-GHz data for this interval were not included because of the difficulty in identifying rain attenuation data; meteorological measurements were not made in conjunction with this experiment.

II. SUMMARY

Highlights of the results detailed in Sections IV thru VIII are given in this section. A few definitions are needed first:

L: Normalized algebraic value of envelope voltage (fade depth in dB $= -20 \log L$)
P: Fraction of time T that the envelope voltage is $\leqq L$
N: Number of fades (during T) of the envelope voltage below L
t: Duration of a fade below L in seconds ($\bar{t}$ = average duration)
f: Frequency in GHz
D: Path length in miles

The major results are:

(*i*) The 11-GHz amplitude statistics for the data base interval (T) of 5.26×10^6 seconds and for fade depths exceeding 15 dB are $P = 0.69L^2$, $N = 12{,}300L$, $\bar{t} = 330L$. Also $t/\bar{t}$ is log-normal and independent of L with 1 percent of the fades at any level longer than ten times the average.

(*ii*) The P and N statistics for the 4- , 6- , and 11-GHz data are, within experimental error, linear functions of frequency given by $P = 0.078fL^2$ and $N = 1000fL$. The comparable $\bar{t}$ statistic is given by $\bar{t} = 410L$.

(*iii*) An empirical estimate of P for the worst fading month is

$$P = rL^2, \qquad L \leqq 0.1$$

where r is defined as the multipath occurrence factor and is given by

$$r = c\left(\frac{f}{4}\right)(D^3)(10^{-5})$$

with

$$c = \begin{cases} 1 & \text{average terrain} \\ 4 & \text{over-water and Gulf Coast} \\ 0.25 & \text{mountains and dry climate.} \end{cases}$$

(*iv*) Of the days in the 1966 Ohio data base, about 12 had more fading than the average while 54 had less. The worst day contained about 48 percent of the total fade time at or below 40 dB while the worst hour contained some 20 percent.

(*v*) The simple model, $P = aL^2$, can be used to characterize shorter periods with multipath fading.* The cumulative empirical probability distribution (c.e.p.d.) with $a \equiv a_d$ is for daily fading

$$\Pr(a_d \geqq A) \cong \exp[-1.2\sqrt{A(4/f)}]$$

and for the hourly fading with $a \equiv a_h$

$$\Pr(a_h \geqq A) \cong \exp[-0.7\sqrt{A(4/f)}].$$

The hourly median fade depth value exceeded by 1 percent of the hours is 18 dB below free space.

(*vi*) The random variable defined as the difference between the median for a minute in a fading hour and the median for the entire hour was found to be normally distributed with zero mean and a standard deviation of 5.5 ± 1.5 dB.

III. EXPERIMENTAL DESCRIPTION[2]

The data presented were obtained by the MIDAS† measuring equipment at West Unity, Ohio. The basic data consist of measurements of the received envelope voltages of standard TD-2 (4 GHz), TH (6 GHz), and TL (11 GHz) signals; Table I is a list of the center frequencies of each channel. A functional block diagram is shown on Fig. 1. The 4-GHz and 6-GHz channels were standard in-service FM radio channels with nominally constant transmitted power (±0.5 dB). The 11-GHz

* The change in the coefficient from r to a is made to clearly differentiate between the total measurement period and the daily (or hourly) epoch.

† An acronym for Multiple Input Data Acquisition System.

TABLE I—RADIO CHANNELS MEASURED AT WEST UNITY, OHIO

Channel No.*	Frequency (MHz)	Antenna	Polarization
4-7	3750	Horn Reflector	V
4-1	3770		H
4-8	3830		V
4-2	3850		H
4-9	3910		V
4-11	4070		V
4-6	4170		H
6-11	5945.2		H
6-13	6004.5		H
6-14	6034.2		V
6-15	6063.8		H
6-17	6123.1		H
6-18	6152.8		V
11-1	10995		V

* The 4-*X* channels correspond to standard TD-2 radio system signals; 6-*X* corresponds to TH; 11-1 corresponds to TL.

channel was added especially for the test program and was unmodulated, with the RF equipment housed in an outdoor cabinet.

West Unity, Ohio, was chosen as the site for this experiment because it is part of a major cross-country route in an area known to suffer multipath fading. The hop monitored was of typical length—28.5

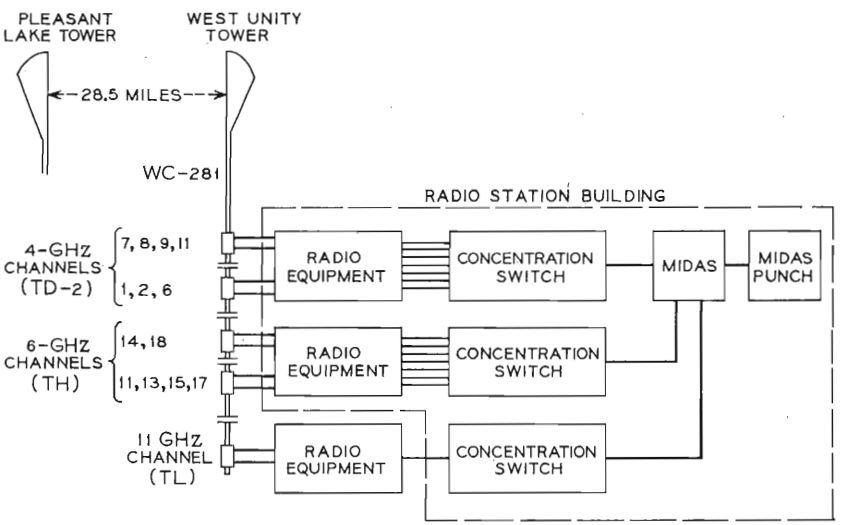

Fig. 1—1966 experimental layout, Pleasant Lake–West Unity.

miles—with negligible ground reflections. The path clearance was adequate even for the extreme of equivalent earth radius (k) equal to two-thirds, as shown on the path profile in Fig. 2. It is believed that this path is typical of those inland paths subject to multipath fading conditions.

The MIDAS equipment sampled each signal five times per second, converted each measurement to a decibel scale, and recorded the data in digital form for subsequent computer processing (in the absence of fading the recording rate was less than the sample rate). Further equipment details are given in Ref. 2.

The data were obtained during the period from 00:28 on July 22 to 08:38 on September 28, 1966. The total elapsed time was 5.9×10^6 seconds of which 5.26×10^6 seconds was selected for the data base; the balance was unusable mainly because of maintenance of the radio equipment or MIDAS. Within the data base, 7.8×10^5 seconds contained all the multipath fading in excess of approximately 10 dB. The balance of the time, 4.48×10^6 seconds, was categorized as nonfading time.

A natural epoch for multipath fading is the 24-hour period from noon to noon. It was convenient to number these periods from 1 to 69 starting at noon on July 21 and ending at noon on September 28. Here the

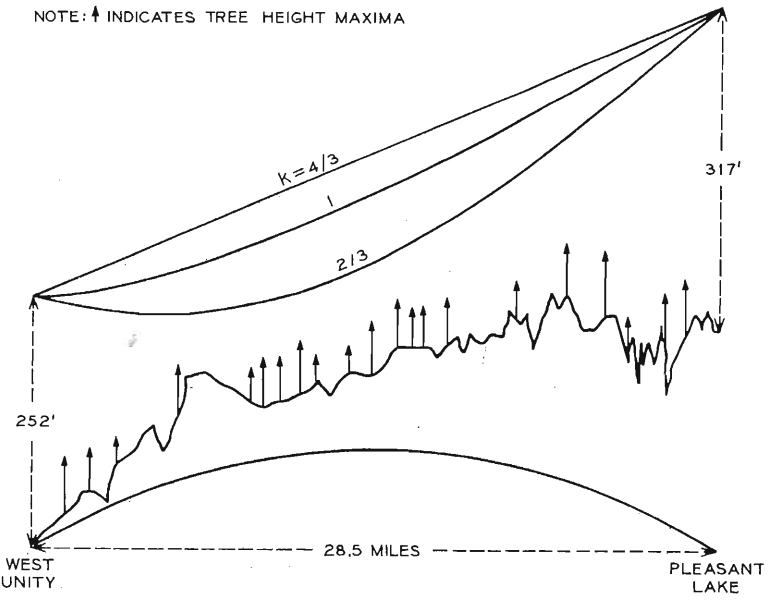

Fig. 2—West Unity–Pleasant Lake path profile.

missing end periods from 12:00, July 21 to 00:28, July 22 and 08:38 to 12:00 on September 28 have been assumed negligible. Most of the multipath fading was found to occur in the period between midnight and 9 A.M. as will be discussed later. These latter time periods were, for all practical purposes, subject to continuous measurement for 66 of the 69 periods. Thus, we reduce the multipath fading data base to 66 nine-hour periods. These were used for channel characterization and for investigating the daily and hourly statistical properties of multipath fading.

All fading distributions will be given in terms of the received voltage relative to the midday normal in dB. The rms variation in the dB reference level was estimated as ± 0.8 dB.[2]

IV. 11-GHz MULTIPATH RESULTS

The 11-GHz data were analyzed in terms of the statistical properties previously reported for the 4- and 6-GHz data.[2,4] These were (*i*) the fraction (P) of 5.26×10^6 seconds that the signal was faded below a given level L, (*ii*) the number of fades (N) below L, (*iii*) the average duration in seconds ($\bar{t}$) of fades below L, and (*iv*) the fade duration distribution. The data were carefully inspected to insure that only multipath fading was included and that rain fading was excluded. This was done by inspection of signal level vs time plots with the determination made by the frequency of the fading and by comparison with the 4- and 6-GHz data. As in the case of the 4- and 6-GHz data, we were most interested in fades greater than 15 dB. However, reliable data for the 11-GHz signal were limited to fade depths of 35 dB because the reference level of received signal strength was 5–10 dB lower than that for the 4- and 6-GHz signals.

The data for the fractional fade time are given in Fig. 3. They are adequately represented by a straight line whose equation is $P = 0.69L^2$. The data for the number of fades are given in Fig. 4 along with the fitted line $N = 12{,}300L$. The data for the average fade duration are obtained from the ratio of the total time faded to the number of fades and are given in Fig. 5 along with the fitted line $\bar{t} = 330L$. These variations of P, N, and $\bar{t}$ with L are in agreement with those previously found for the more extensive 4- and 6-GHz data and are as predicted from a mathematical model of the multipath fading process.[7]

The probability that a fade of depth $-20 \log L$ dB lasts longer than t seconds, i.e., the fade duration distribution, can be estimated by dividing the number of fades of depth L and duration t seconds or longer by the total number of fades of depth L. A normalization is made

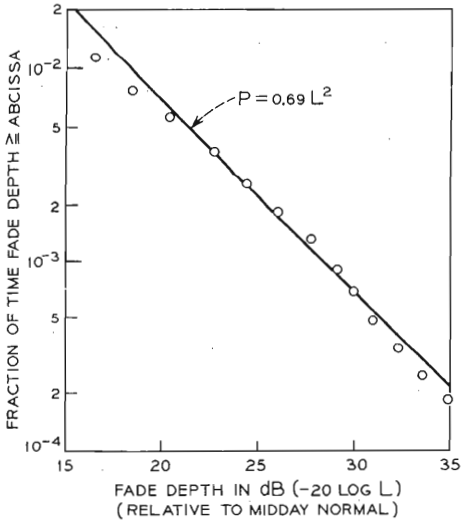

Fig. 3—11-GHz fade depth distribution, 1966 West Unity.

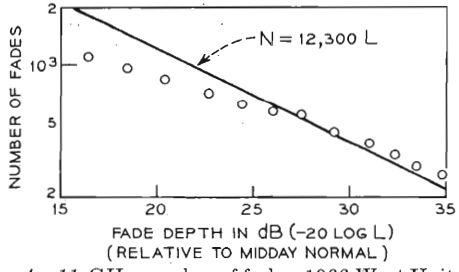

Fig. 4—11-GHz number of fades, 1966 West Unity.

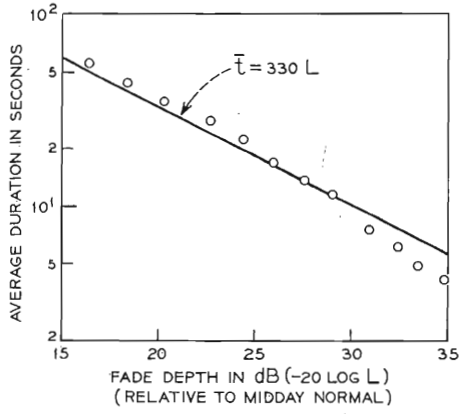

Fig. 5—11-GHz average fade duration, 1966 West Unity.

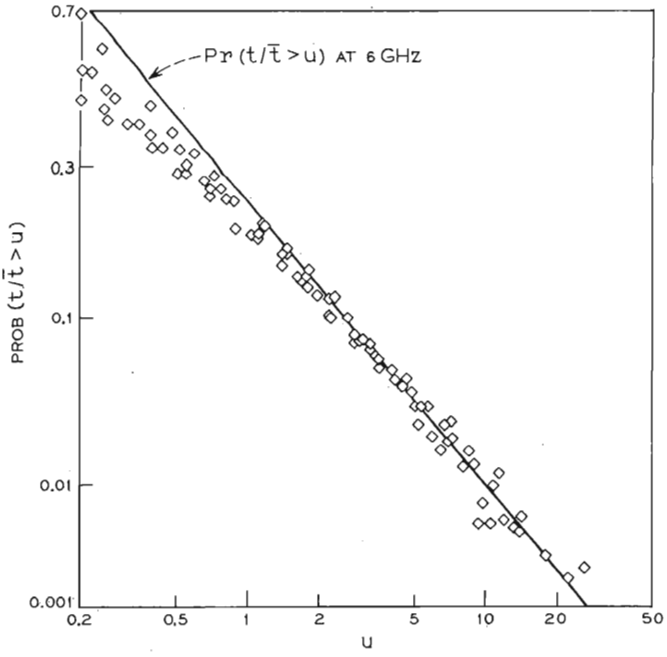

Fig. 6—11-GHz fade duration distribution: probability that the fade duration, normalized to its mean for a given fade depth, is longer than a given number. Data pooled for all fade depths greater than 10 dB.

with respect to the average fade duration. The 11-GHz data are plotted on Fig. 6, using a normal probability scale, for all fades $\geqq 10$ dB. The data indicate that $t/\bar{t}$ is independent of L and that the probability is approximately log normal with 1 percent of the fades being longer than ten times the average fade duration. The line on Fig. 6, taken from Fig. 40 of Ref. 4, represents the fade duration distribution for the corresponding 6-GHz data. Thus, the fade duration distributions, when properly normalized, appear to be invariant with frequency.

V. MULTIPATH EFFECTS AS A FUNCTION OF FREQUENCY

The 11-GHz results of Section IV can be combined with those previously obtained for 4 and 6 GHz[2,4] to obtain an estimate of the variation of the characteristics with microwave frequency. This treatment is valid because all the data were obtained under identical conditions: same path, same antennas,* and same time period.

* The different beamwidths of the horn reflector for the three frequencies play a minor role because the variations in angle-of-arrival of the multipath components are generally less than the smallest beamwidth, which is ± 0.6 degree at 11 GHz.

TABLE II—MULTIPATH FADING CHARACTERISTICS
($L \leqq 0.1$)

Freq (GHz)	P	N	$\bar{t}$
4	$0.25L^2$	$3670L$	$408L$
6	$0.53L^2$	$6410L$	$490L$
11	$0.69L^2$	$12300L$	$330L$

Table II summarizes the 4-, 6-, and 11-GHz results. The tabulated coefficients incorporate the effects of the environment and frequency. Plotting them versus frequency (as in Fig. 7) allows us to observe that the N and P coefficients increase, within experimental error, linearly with f while $\bar{t}$ is longer at 6 GHz and shorter at 11 GHz with respect to 4 GHz. Based upon these data, an approximation that $\bar{t}$ is independent of f is reasonable. The functional dependence is described by:

$$P = 0.078fL^2, \tag{1}$$

$$N = 1000fL, \tag{2}$$

$$\bar{t} = 410L, \tag{3}$$

with f in GHz.

The deviation of the P and N coefficients of Table II from these empirical equations is less than ± 1 dB which is within the bounds of experimental error.[2] The $\bar{t}$ coefficients agree with equation (3) within ± 2 dB. This is satisfactory since the $\bar{t}$ data were originally obtained as the ratio of the P and N data at each fade level; ± 1 dB variation each in P and N corresponds to ± 2 dB variation in $\bar{t}$.

The multiple transmission paths which give rise to the fading effects are generated by irregularities in the refractivity gradient in the volume defined by the beamwidths of the two antennas. As the relative path lengths vary with time the composite received signal may fade due to destructive interference (or be enhanced by constructive interference). It is easy to see that a given change in relative path length will cause more signal variations at higher frequencies because of the proportionally larger phase variations; we have found that the effect in Ohio in 1966 was linear. There is no apparent reason why this variation with frequency does not generally apply for multipath fading for a normal overland path engineered in standard fashion. Also, a linear variation of P with frequency has been theoretically predicted by C. L. Ruthroff[6] from a careful analysis of a simple physical model of multipath fading.*

* The results discussed here predate Ruthroff's analysis.

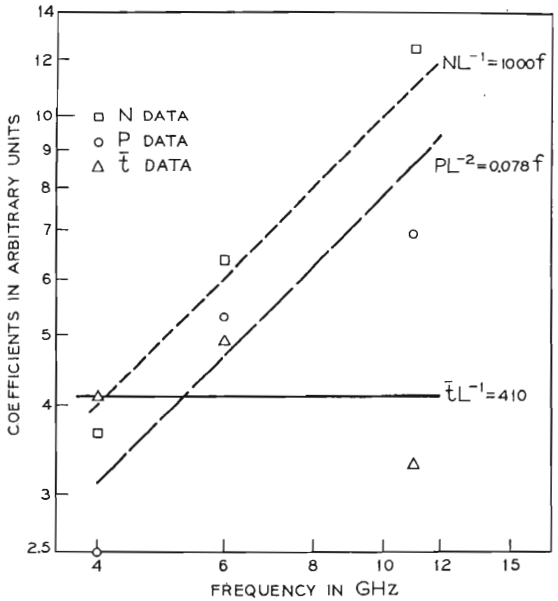

Fig. 7—Coefficients of P, N, and $\bar{t}$ characteristics versus frequency.

VI. OCCURRENCE OF MULTIPATH FADING

6.1 *General*

It is well known that the time (probability) distribution of the envelope of a microwave signal subject to multipath fading depends upon path length, path geometry, terrain clearance, type of terrain, and meteorological conditions in a complex manner. A general treatment of these relationships is intractable. However, based on the results discussed in previous sections and in other papers, an engineering estimate (incorporating the most important factors) of the fade depth distribution can be made for typical microwave paths for the heavy fading time of the year, i.e., the so-called worst month fading. In the results that follow adequate path clearance and negligible ground reflections are assumed.

6.2 *Relation to the Rayleigh Distribution*

Quite often in propagation studies it is assumed that the probability distribution of the envelope (v) of the received signal is given by the Rayleigh formula

$$\Pr(v < L) = 1 - e^{-L^2} \cong L^2 \quad \text{for} \quad L < 0.1. \tag{4}$$

One physical basis of this distribution is the limiting case of the envelope of an infinitely large number of equal amplitude signals of the same frequency, but random phase. Since this is a good approximation in many situations, e.g., tropospheric and mobile radio propagation, this distribution has seen much use. In the case of line-of-sight microwave radio, this is not a good assumption and the distribution is not directly applicable. From Table II the results for the fade depth distribution P vary as L^2 but with different coefficients.* The coefficient is generally not fixed, but depends upon the time base of the data, and upon the particular path parameters. The path parameters can be incorporated in the coefficient by expressing the multipath fade depth distribution as

$$\Pr(v < L) = rL^2 \qquad L < 0.1 \tag{5}$$

where r is defined as the multipath occurrence factor; $r = 1$ is appropriate to the Rayleigh distribution.

6.3 *Path Parameters*

As discussed in Section V, r is directly proportional to frequency; terrain and distance effects have to be incorporated. An engineering estimate for r can be given as a product of three terms†

$$r = c\left(\frac{f}{4}\right)D^3 10^{-5} \tag{6}$$

where: f is frequency in GHz,
D is the path length in miles,

$$c = \begin{cases} 1 & \text{average terrain} \\ 4 & \text{over-water and Gulf Coast} \\ 0.25 & \text{mountains and dry climate.} \end{cases}$$

The terrain effects and the distance dependence are based on applicable (albeit meager) Bell System data, most of which was acquired at 4 GHz on paths of 20–40 miles length. The plot given on Fig. 8 extends beyond this range. Indeed it can be argued that the curves should become parallel to the abscissa as D decreases (no multipath fading for paths sufficiently short[6]) and parallel to the ordinate (saturation) as D increases.

* An analysis of a mathematical model for multipath fading shows that the deep fade region of the distribution will be proportional to L^2 under very general conditions (Ref. 7).

† This empirical result for r is partially supported by British data as reported by K. W. Pearson[8] and is similar to a concise result reported by S. Yonezawa and N. Tanaka.[9]

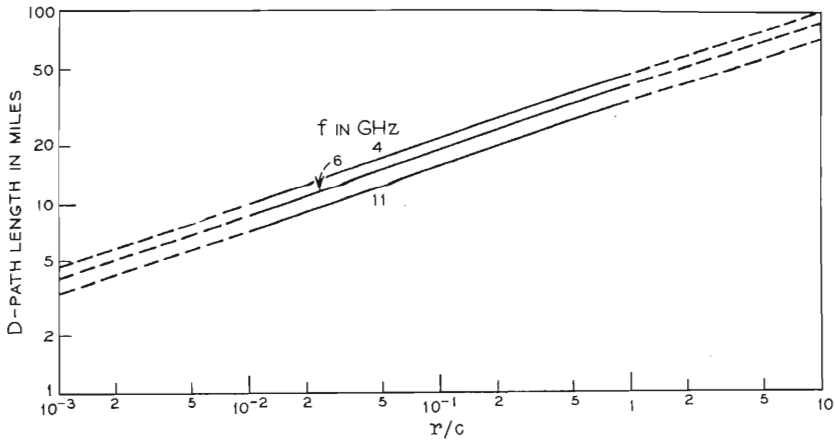

Fig. 8—Worst month multipath fading: $P = rL^2 = c(f/4)\,D^3L^2$.

The plotted values are certainly upper bounds for either extreme. The fD^3 dependence has been theoretically obtained by Ruthroff.[6]

The engineering estimate, equation (6), indicates that on a path of above average length, maintenance of the per-hop fading outage usually obtaining requires compensation for the additional free-space loss ($\propto D^2$) and for increased multipath ($\propto D^3$), which combine to impose a D^5 (15 dB/octave) length dependence.

VII. TIME CONCENTRATION OF DEEP MULTIPATH FADING

7.1 *Introduction*

The results and estimates already given utilize the entire data base, thus averaging temporal effects. It is well established that multipath fading occurs most often at night, with a few nights experiencing considerably more fading than most of the others. Describing this variability statistically is the objective here. We consider the fade time statistic for hourly and for daily periods and the median fade depth during an hour or a minute.

The analysis includes data from four fade depth values,* 9.8 dB, 20.4 dB, 31 dB, and 40.1 dB (henceforth labeled as levels 1 through 4). At each fade depth and for each analysis period the fade time for the seven 4-GHz channels was arithmetically averaged, as was that for the six 6-GHz channels. The fade time for the 11-GHz channel was used

* The unusual numbers are the result of quantization and calibration.[2]

TABLE III—FADE TIME DATA
(Seconds at or Below Given Fade Depth)

Freq Band (GHz)	Fade Depth 1 (9.8 dB)	2 (20.4 dB)	3 (31 dB)	4 (40.1 dB)
4	148,427	13,771	1329	135
6	259,933	27,503	2562	312
11	243,977	32,232	2982	*

* No data was obtained at 11 GHz for fade depth 4; see Section IV for further details.

directly. The resulting data will be referred to as the 4-, 6-, and 11-GHz fade times respectively. The fade time totals for the entire test period (5.26×10^6 seconds) are given in Table III.

7.2 *Distribution by Days—Rank Order Data*

The fade times for fade depths 1–4 were separately compiled for each of the 66 noon-to-noon periods. As expected there is considerable variation. As an example, Fig. 9 shows a plot of the 6-GHz fade time versus day number. Here the value plotted is the ratio of the fade time for the day to the total fade time, given in Table III, for a fixed fade depth. Much of the deep fading (levels 2, 3, 4) occurred on days 10,

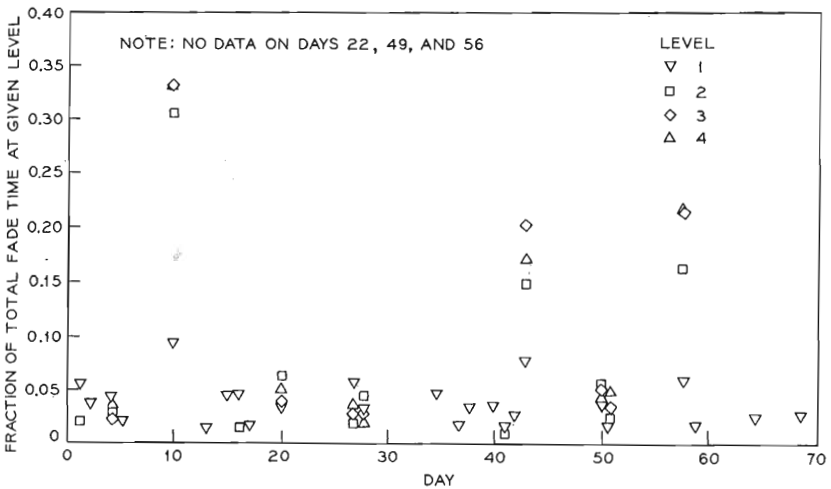

Fig. 9—Daily variation of multipath fading at 6 GHz, 1966 West Unity.

43, and 58 while the fading time for level 1 was more widely distributed.

The days were separately rank ordered for each frequency and each level with the variable again being the fraction of the total fade time; the results are given on Figs. 10a–c.* A few observations from these plots:

(*i*) The worst day fraction increases with level.
(*ii*) The data for level 1 do not fall off as rapidly with rank order as for levels 2–4.
(*iii*) Long tails in the rank order are prevalent.

Some of the more pertinent statistics are summarized in Table IV.

As already noted from Fig. 9, the bulk of the deep fading occurred on three days (10, 43, 58). The fraction of the total fading at the sample levels summed for these three days ranges from 0.55 to 0.74. Day 10 was the worst day in all cases. It appears that if a day suffered extensive 20-dB fading it also suffered 30- and 40-dB fading, but this indicator is not valid for 10-dB fading. In fact, about two-thirds of the days had 10-dB fading while only one-third had some 40-dB fading.

The statistical worst night is of particular interest. Figure 11 is based upon the observation that the worst day fraction increases with fade depth. The data points are fairly consistent except for levels 3 and 4 at 6 GHz which, for some unknown reason, do not show the expected increase relative to level 2. The line on Fig. 11 can be used as an estimate of the worst day fraction as a function of level. This estimate predicts that for systems with 40-dB fade margins the worst day will have 48 percent of the total fading within the worst month.†

A different perspective on the daily fading time can be obtained from Figs. 12a–c, which replot the rank order data on a logarithmic scale which has the effect of emphasizing the tail behavior. Generally, the tail is longer for lesser fade depths. It is interesting to compare these data with the result that would obtain for a uniform fade time distribution: a horizontal line at 0.015 (1/66). This line intercepts the level 2, 3, 4 data in the range of 10–15 days which means that this number of days had more fading than the average for the entire period while some 51–56 days have less fading. We shall return to the daily data in a later section where we shall see that they can be reduced to a more

* The data were plotted for all the days such that the cumulative sum of the plotted fade times just exceeded 99 percent of the total; note change of scale at rank order day 5.

† Here we take our statistics as representative of the worst month, the argument being that our results for a late summer—early fall period are generally comparable to the so-called worst fading month in a year.

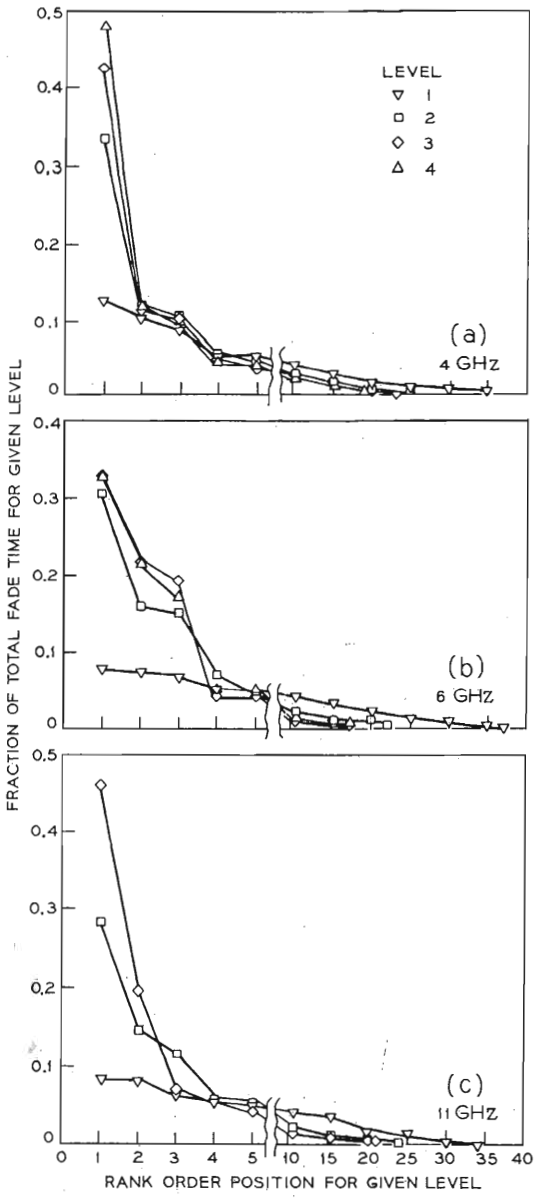

Fig. 10a—Rank order of 4-GHz daily fade times, 1966 West Unity.

Fig. 10b—Rank order of 6-GHz daily fade times, 1966 West Unity.

Fig. 10c—Rank order of 11-GHz daily fade times, 1966 West Unity.

TABLE IV—DAILY FADE TIME STATISTICS

Freq (GHz)	Level	Number of Days With Fade Time >0	Fraction of Total Fade Time		Number of Days to Give 0.99 of Total
			Worst Day	Sum of 3 Worst Days	
4	1	46	0.125	0.31	35
	2	36	0.33	0.56	25
	3	30	0.43	0.64	23
	4	26	0.48	0.70	19
6	1	46	0.077	0.22	37
	2	35	0.30	0.61	22
	3	27	0.33	0.73	17
	4	24	0.33	0.71	16
11	1	43	0.083	0.22	34
	2	35	0.29	0.55	24
	3	30	0.47	0.74	21

meaningful form given the appropriate statistical treatment and mathematical modeling.

7.3 *Distribution by Hours—Rank Order Data*

The preceding treatment on daily fade time is repeated here for hourly fade time. This fade time is expressed as a fraction of all time during the entire measurement period as given in Table III. Of course, greater scatter can be expected in the hourly data than in the daily data.

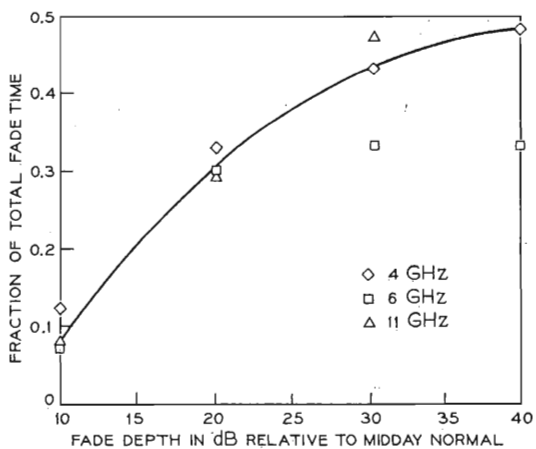

Fig. 11—Fraction of total fade time in worst night, 1966 West Unity.

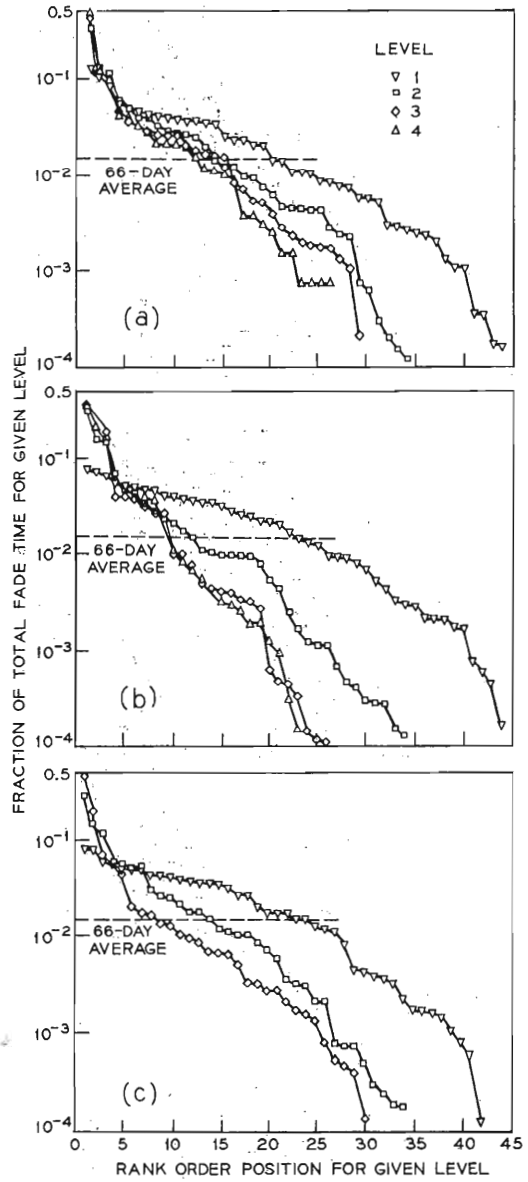

Fig. 12a—4-GHz rank order of daily fade times, 1966 West Unity.

Fig. 12b—6-GHz rank order of daily fade times, 1966 West Unity.

Fig. 12c—11-GHz rank order of daily fade times, 1966 West Unity.

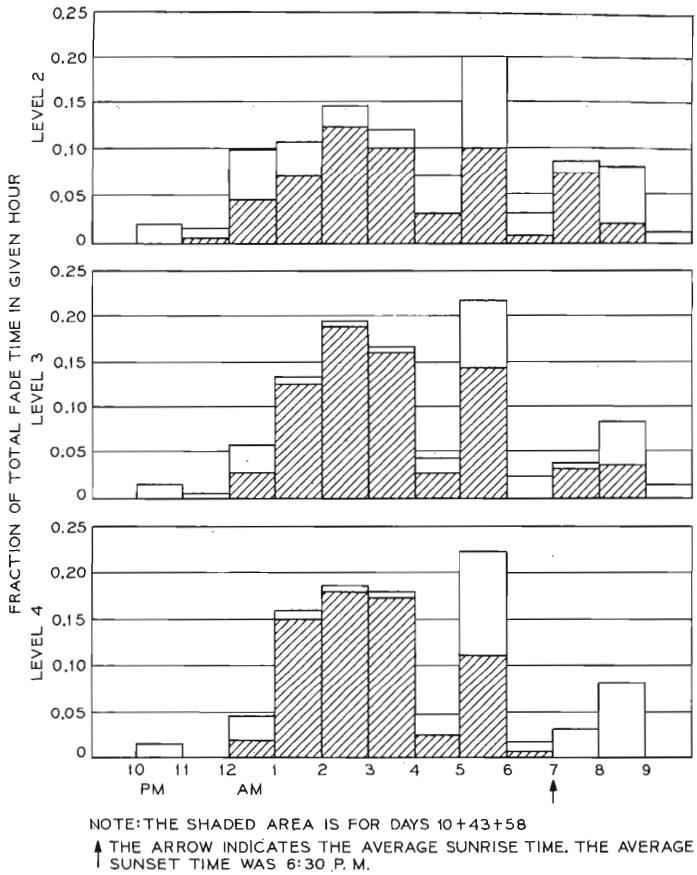

Fig. 13—6-GHz hour-of-day ranking, 1966 West Unity.

Figure 13 shows the distribution of fading for levels 2, 3, and 4 for the 6-GHz channels as a function of the hour of the day. Deep fading was generally within a 9-hour period between 12 P.M. and 9 A.M. The hours were rank ordered by level within a particular frequency band as shown on Figs. 14a–c. The general observations that can be made are similar to the "days" case:

(*i*) The worst night fraction increases with fade depth.
(*ii*) The level 1 fraction does not fall off very rapidly.
(*iii*) Long tails are even more prevalent than for daily fading.

Some of the pertinent statistics are summarized in Table V.

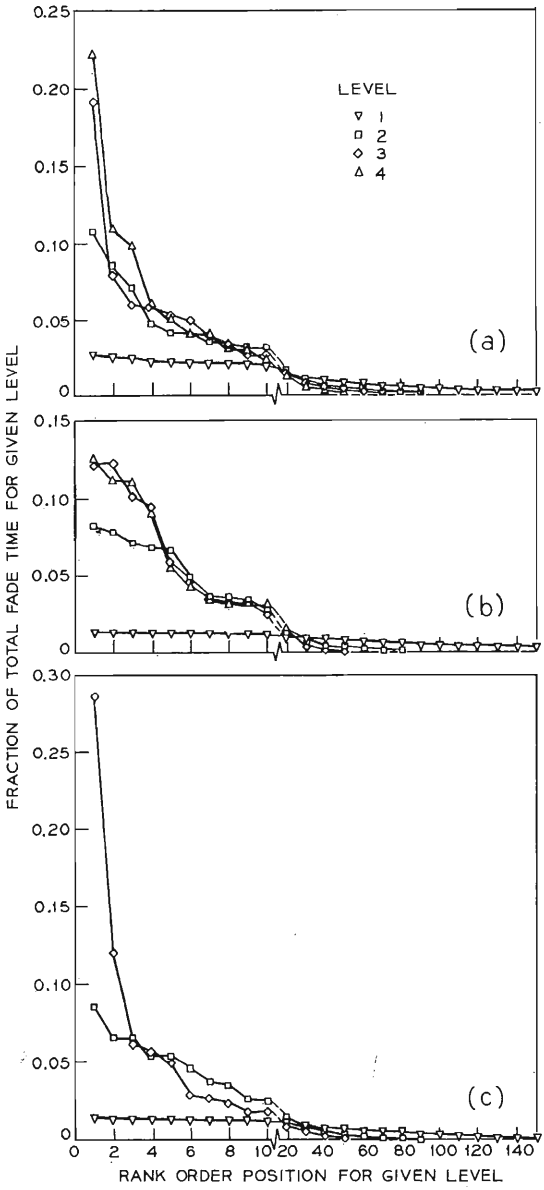

Fig. 14a—4-GHz rank order of hourly fade times, 1966 West Unity.

Fig. 14b—6-GHz rank order of hourly fade times, 1966 West Unity.

Fig. 14c—11-GHz rank order of hourly fade times, 1966 West Unity.

TABLE V—HOURLY FADE TIME STATISTICS

Freq (GHz)	Level	Number of Hours	Fraction of Total Fade Time		Number of Hours to Give 0.50 0.90 0.99 of Total Fade Time		
			Worst Hour	10 Worst Hours			
4	1	220	0.027	0.226	33	103	163
	2	117	0.107	0.525	10	48	80
	3	88	0.192	0.621	7	36	69
	4	61	0.222	0.699	5	24	47
6	1	259	0.014	0.128	50	138	206
	2	123	0.083	0.559	9	39	83
	3	78	0.123	0.681	5	24	49
	4	56	0.126	0.672	6	22	43
11	1	230	0.015	0.136	48	127	189
	2	121	0.085	0.495	11	46	88
	3	70	0.286	0.694	4	28	53

The worst hour for each transmission band is plotted versus fade depth in Fig. 15. The data spread is greater than for the days case (Fig. 11) with 6 GHz again exhibiting the least variation. The line on Fig. 15 can be used as an estimate of the worst hour fraction as a function of level. Thus, the worst day (Fig. 11) and worst hour (Fig. 15) estimates

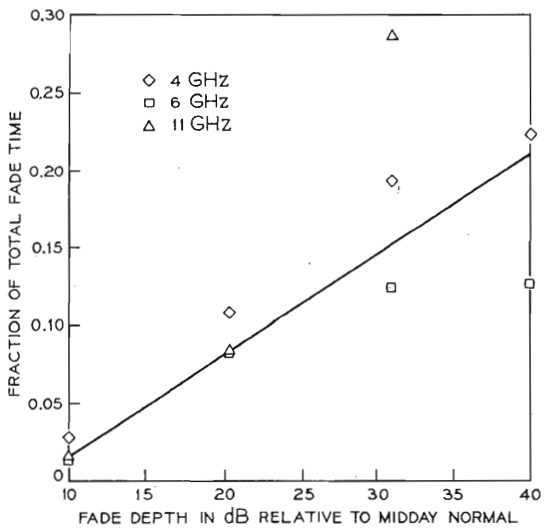

Fig. 15—Fraction of total fade time in worst hour, 1966 West Unity.

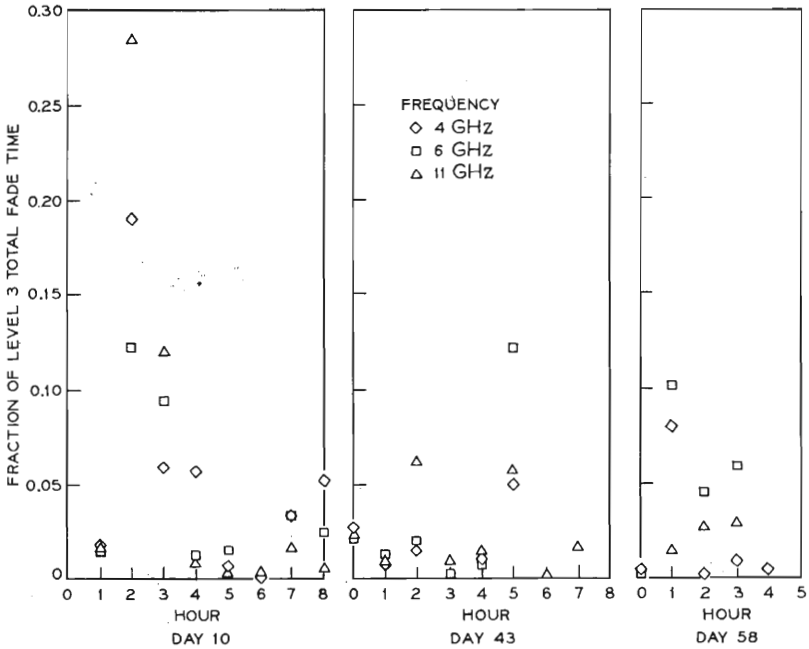

Fig. 16—Fraction of total fade time: level 3 hourly variation on three worst days.

for 40 dB predict 48 percent of the worst month multipath in a single day with 21 percent in the worst hour.

Days 10, 43, and 58 merit special study since they contain a majority of the deep fade time. The hourly variation in fade time for level 3 is given on Fig. 16. It is obvious from these data that there is no fixed relation between the frequency bands on an hourly time scale.* The hour from 2 A.M. to 3 A.M. on day 10 was the worst hour with the fractional fade time ranking with frequency as 11–4–6. However, the hour from 5 A.M. to 6 A.M. on day 43 was also a bad one with the fractional fade time ranking with frequency as 6–11–4. On day 58 the hour from 1 A.M. to 2 A.M., which was also outstanding, had the frequency order 6–4–11. However, the overall statistics show that fading severity increases with frequency.

7.4 *Hourly Median for a 4-GHz Channel*

The data reported in previous sections were in terms of the fraction of time that some fixed fade depth was exceeded; a reversal of these

* This conclusion does not change if absolute fade time is used instead of fractional fade time.

roles is equally valid. The variable examined in this section is the fade depth exceeded for a total of 30 minutes in an hour (hourly median). Figure 17 shows a rank order of the hourly median data for one of the 4-GHz channels as obtained directly from the experimental data for each hour. This particular channel is considered typical. The worst hourly median was 20.5 dB below free space and some 10 hours had hourly medians in excess of 15 dB. The general tendency is quite regular and shows a slowly decreasing median value with 120 hours experiencing hourly median fades in excess of 5 dB.

7.5 *Analytic Model for Hourly Median*

The single-channel fade depth statistics have a common characteristic: the fractional probability that the signal v is at or below L is proportional to L^2 (see Table II). Lin[7] has shown that this is a general property of fading signals under very general conditions, i.e.,

$$P \equiv \Pr(v \leqq L) = aL^2 \equiv \frac{t_L}{T} \qquad L \leqq 0.1 \tag{7}$$

where a is an environmental constant and t_L/T is the fractional fade time for the time period T.

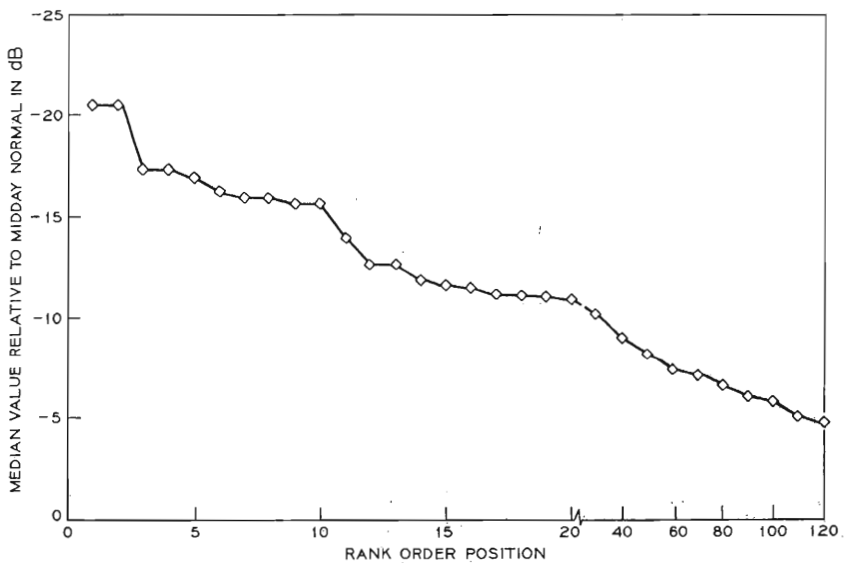

Fig. 17—4-GHz rank order of hourly median (channel 4–7).

This formula will be used here with the following modification for analytical simplicity,

$$P = \Pr(v \leqq L) = \begin{cases} aL^2 = \dfrac{t_L}{T} & 0 \leqq L^2 \leqq \dfrac{1}{a} \\ 1 & L^2 \geqq \dfrac{1}{a} \end{cases} \tag{8}$$

For this simple model the median value, L_m, is given by

$$L_m^2 = \frac{1}{2a} = \frac{L^2 T}{2t_L}. \tag{9}$$

This relation can be used to calculate values of L_m from the 4-GHz hourly rank order data of Fig. 14a. The results for levels 2 and 3 are shown on Fig. 18 along with the 4-GHz hourly median data from Fig. 17. There is good agreement for the first 20 rank order days. Level 3 predicts a worst hour median 2.5 dB higher and level 2 predicts a worst hour median 1 dB lower than the Fig. 17 data.

The calculated results roll off faster below 10 dB than the Fig. 17 data, which means that the aL^2 model does not hold when the hourly median is less than 10 dB. This is to be expected because the aL^2 model applies for multipath fading while the Fig. 17 data contains a con-

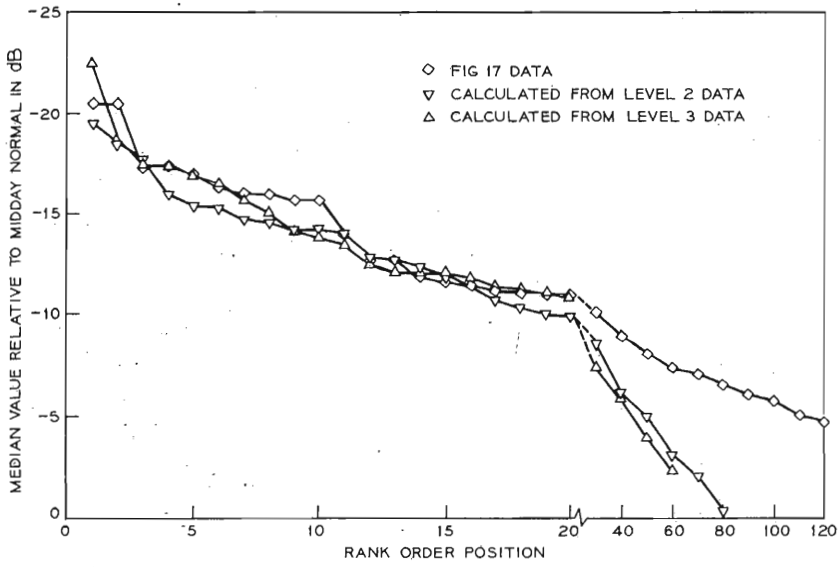

Fig. 18—Comparison of 4-GHz hourly median data of Fig. 17 with calculated values.

siderable number of hours during which the signal is depressed with little multipath fading. In any case, the analytic model (8) is adequate for the higher values of the hourly median which is the region of greatest interest. This model will now be applied to the nightly and hourly rank order data presented in Figs. 10 and 14.

7.6 *Empirical Probability Distribution of Daily Fade Time*

The rank order data (Section 7.2) can be used to estimate the probability distribution for the daily fade time by plotting the value of the ith ordered sample versus the probability estimate $(N)^{-1}\ (i - 0.5)$, defined as the cumulative empirical probability distribution (c.e.p.d.).[10] The random variable t_L is defined as the total amount of time during the 9-hour period for which the signal level is less than or equal to L.* The rank order daily fade time data (Section 7.2) are samples of t_L, with t_{Li} the ith rank ordered sample value. Thus the c.e.p.d. is:

$$P_{Li} \equiv \Pr\,(t_L > t_{Li}) = \frac{i - 0.5}{N_L} \tag{10}$$

where N = number of sample values.

Repeating equation (7) in a form consistent with the above definitions gives

$$\Pr\,(v_i \leqq L) = a_i L^2 = \frac{t_{Li}}{T_d} \tag{11}$$

where v_i is the envelope voltage during the ith interval,
a_i is the environmental constant during the ith interval,
T_d = 9 hours.

Combining (10) with (11) gives

$$P_{Li} = \Pr\left(\frac{t_L}{L^2 T_d} \geqq \frac{t_{Li}}{L^2 T_d}\right) = \Pr\,(a_d \geqq a_i). \tag{12}$$

Thus the c.e.p.d. for t_L is identical to that for the random variable a_d, the daily environmental constant.

In the calculation of P_{Li} for levels 2–4 the values used for N_L will be those given in Table IV. At level 2 there were 36 days with non-zero fade time at 4 GHz and 35 at both 6 and 11 GHz. If the aL^2 model is interpreted in a deterministic sense then all days with level 2 fade time should have level 3 fade time; yet there were only 30 such days at 4 GHz.

* The 9-hour period was chosen because most of the daily fading occurred between 12 P.M. and 9 A.M.

There is no inconsistency because the aL^2 model is statistical so that not all level 2 fades also generate level 3 fades; thus the 30 samples are used to construct a c.e.p.d. which can be compared to that obtained for the 36 samples at level 2. The corresponding procedure was followed for level 4 at 4 GHz and for levels 2–4 for 6 and 11 GHz. Two basic assumptions are made: (*i*) 0.2-second sampling has a negligible effect; (*ii*) the samples at any level are independent. The first assumption will be justified if the level 4 results are consistent with the level 2 results because the sampling interval would have a greater effect on the level 4 results. The second assumption only requires independence from day to day which is plausible.

The daily rank order fade time data have been plotted on Figs. 19a–c according to (12). The probability scale is exponential and the abscissa is logarithmic. The data for all three frequencies appear to be independent of level and approximately linear with increasing scatter above 70 percent. The conclusion is that the aL^2 representation is adequate over the 20–40 dB fade depth range for daily fading.

In Section V we examined the frequency dependence of the environmental constant. Utilizing that relation, and normalizing to 4 GHz, equation (12) becomes:

$$P_{Li} = \Pr\left[\frac{a_d}{\left(\frac{f}{4}\right)} \geqq \frac{a_i}{\left(\frac{f}{4}\right)}\right]. \tag{13}$$

The level 2 data for 4, 6, and 11 GHz has been plotted in Fig. 20 according to (13). The reduced data are consistent for the three frequencies; a straight line whose equation is

$$\Pr\left(\frac{t}{L^2T_d} = a_d \geqq A\right) = \exp\left(-1.2\sqrt{A\left(\frac{4}{f}\right)}\right) \tag{14}$$

provides a good fit (±2 dB) to the data below 0.9. Similar results are obtained for levels 3 and 4 but with increased scatter.

Figure 20 indicates that the environmental parameter a_d is linearly dependent on frequency on a day-to-day statistical basis for multipath fading. This is a stronger result than that of Section V, where the linear frequency dependence was found valid for the measurement period taken as a whole. The net result of this analysis is that the daily fade time for a day picked at random can be calculated statistically.

The result, (14), can be checked against the results given in Table II for the entire measurement period in the following manner. Equation (11) gives, for the ith fading day out of N,

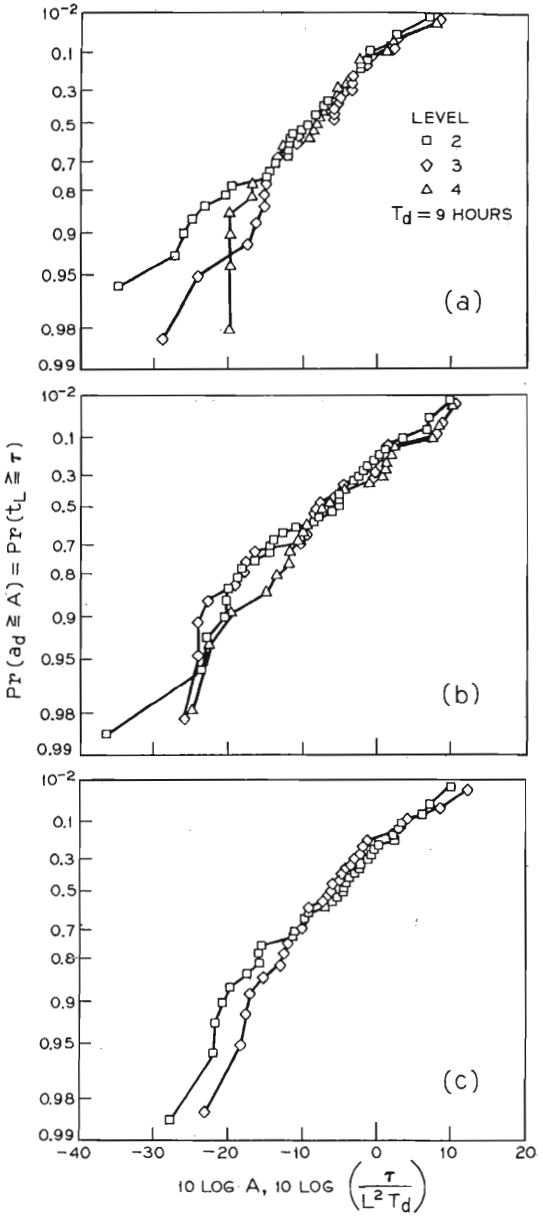

Fig. 19a—4-GHz daily fade time, 1966 West Unity, cumulative empirical probability distribution.
Fig. 19b—6-GHz daily fade time, 1966 West Unity, cumulative empirical probability distribution.
Fig. 19c—11-GHz daily fade time, 1966 West Unity, cumulative empirical probability distribution.

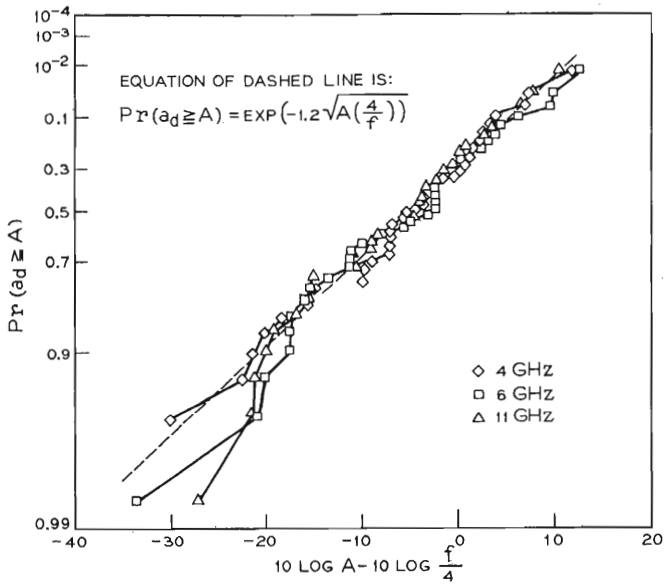

Fig. 20—Daily fade time for level 2, cumulative empirical probability distribution, 4, 6, and 11 GHz, 1966 West Unity.

$$\Pr(v_i \leqq L) = a_i L^2 = \frac{t_{Li}}{T_d}. \tag{11}$$

The fractional fade time accumulated over the N days is [equation (5)]

$$\Pr(v \leqq L) = r_N L^2 = \frac{\sum_{i=1}^{N} t_{Li}}{NT_d} = \frac{\sum_{i=1}^{N} a_i L^2 T_d}{NT_d}. \tag{15}$$

Thus

$$r_N = \frac{\sum_{i=1}^{N} a_i}{N} \tag{16}$$

so that r_N is the average value of the a_i's which in turn can be calculated from

$$P(a_d \leqq A) = 1 - \exp\left(-1.2\sqrt{A\left(\frac{4}{f}\right)}\right). \tag{17}$$

Thus

$$r_N = \int_0^\infty ap(a)\,da = \int_0^\infty a\frac{dP}{dA}\,da \tag{18}$$

$$= 1.4\left(\frac{f}{4}\right).$$

To convert from N periods of 9 hours each to the entire measurement period of 5.26×10^6 seconds the above result must be multiplied by $[(N)(32,\ 400)/5.26 \times 10^6]$. Substitution of the number of days with nonzero level 2 fade time (Table IV) gives the results shown in Table VI. The coefficients obtained from the daily fade times are in fair agreement with the overall coefficients which is a reassuring check on the consistency of the results.

As a digression it is to be noted that the usual Rayleigh assumption for modeling the propagation medium corresponds to $A = 1$. Equation (18) shows that the average value of a_d corresponds to $A = 1.4$. It appears that the Rayleigh assumption is reasonable on the average but it should be recognized that some 30 percent of the days will have greater fading.

The calculation of the daily median is the last topic in this section. As noted in Section 7.5, the median value L_m for the aL^2 distribution model is given as

$$L_m^2 = \frac{1}{2a} \tag{19}$$

or

$$20 \log L_m = -10 \log a - 3 \text{ dB}. \tag{20}$$

Values for 20 log L_m can be read off directly from Fig. 20, e.g., at 4 GHz the 90-percent point is —8 dB relative to midday normal, while the 1-percent point is —14 dB. This calculation is valid only for median values less than some —10 dB because as the value of a gets small the

TABLE VI—FADE TIME COEFFICIENT OF L^2

Freq (GHz)	Calculated from Daily Fade Time	Measured (Table II)
4	0.3	0.25
6	0.45	0.53
11	0.82	0.69

calculated median values will be much too high. This occurs because the range of validity of the aL^2 representation certainly does not extend above -10 dB relative to midday normal. As a matter of fact, the daily median is uninteresting and is included here only for completeness. The next section will take up the matter of the hourly variation for which the median calculation is more meaningful.

7.7 *Empirical Probability Distribution of Hourly Fade Time*

The treatment of the daily fade time in Section 7.6 will be applied to the hourly fade time in this section. As in Section 7.6, we define*

- t_L total time during an hour for which the signal level is less than or equal to L,
- t_{Li} ith rank ordered sample value,
- N_L number of samples,
- v_i envelope voltage during ith hour,
- a_i environmental constant for the ith hour,
- T_h one hour (3600 seconds).

The cumulative empirical probability distribution for the hourly data is constructed according to (see Section 7.6)

$$P_{Li} \equiv \frac{i - 0.5}{N_L} = \Pr\left(\frac{t_L}{L^2T_h} \geqq \frac{t_{Li}}{L^2T_h}\right) = \Pr\,(a_h \geqq a_i) \tag{21}$$

with

$$\Pr\,(v_i \leqq L) = a_iL^2 = \frac{t_{Li}}{T_h}. \tag{22}$$

The hourly rank order data on Figs. 14a–c are replotted on Figs. 21a–c according to equation (21). The probability scale is exponential and the abscissa is logarithmic. The 4-GHz results on Fig. 21a are consistent with less than 3 dB scatter from 0.8 to 0.01 and increasing scatter for smaller data values. The cutoff value imposed by the 0.2-second sampling rate is -22.2 dB for level 2, -11.6 dB for level 3, and -2.5 dB for level 4. Since the 4- and 6-GHz data is averaged for 7 and 6 channels respectively, the actual cutoff point is some 8 dB lower. In any case increased scatter is to be expected for smaller sample values.

The 6-GHz results on Fig. 21b are consistent for levels 2 and 3 but the level 4 data is offset. If all the sample hours had the same amount of fade time at a given level then the c.e.p.d. would be a vertical line on Fig. 21b. One possible explanation, therefore, is that the level 4 hours

* The hourly data utilizes similar notation to that for the daily data.

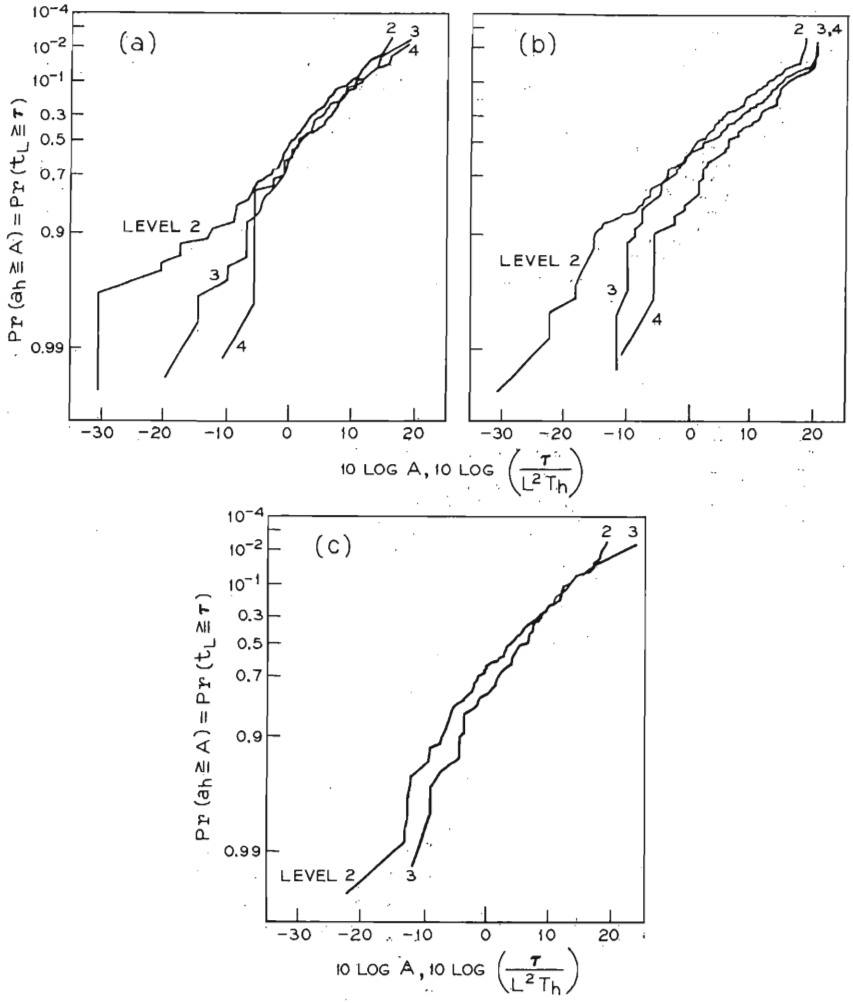

Fig. 21a—4-GHz hourly fade time, 1966 West Unity, cumulative empirical probability distribution.
Fig. 21b—6-GHz hourly fade time, 1966 West Unity, cumulative empirical probability distribution.
Fig. 21c—11-GHz hourly fade time, 1966 West Unity, cumulative empirical probability distribution.

at 6 GHz tended to be more alike than the level 2 and level 3 hours. This behavior was also noted in conjunction with Figs. 14b and 15. We assume that the 6-GHz hourly data for level 4 is atypical.

The 11-GHz results on Fig. 21c are reasonably consistent. Since

there was only one 11-GHz channel, the effect of the 0.2-second cutoff is clearly discernible.

The level 2 data from Figs. 21a–c is cross-plotted on Fig. 22 where the frequency has been normalized to 4 GHz. Thus, assuming that the level 2 data is typical, it is found that the distribution of the hourly environmental constant a_h for hours containing level 2 fades is approximately given by

$$P(a_h \leqq A_h) = 1 - \exp\,(-0.7[A(4/f)]^{1/2}). \tag{23}$$

The square-root function in the exponent was arbitrarily chosen to agree with the result for the daily data, e.g., (14). A slightly larger value than 0.5 would give a better fit for the smaller sample values but this was considered unimportant.

From equation (23), the 50-percent point for 4 GHz falls at $A_h = 1$, with the 99-percent point at $A_h = 30$. This means that for a fading hour the level 2 fade time will exceed 1080 seconds with 1 percent probability.

The hourly median can now be obtained based on the aL^2 model (see Section 7.3):

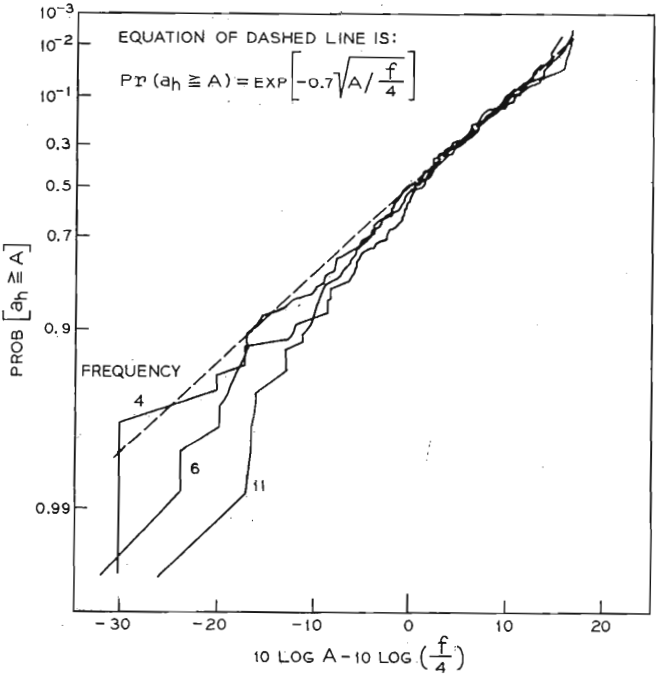

Fig. 22—Hourly fade time for level 2, cumulative empirical probability distribution, 4, 6, and 11 GHz, 1966 West Unity.

$$20 \log L_{mh} = -10 \log a_h - 3 \text{ dB}. \tag{24}$$

Values for L_{mh} can be obtained from Fig. 22 using (24). For example, at 4 GHz the 1-percent median is −18 dB relative to midday normal. The actual maximum data point shown, however, falls at 10 log A = 17 dB which gives a median of −20 dB. This is in good agreement with the minimum median of −20.5 dB for the data given on Fig. 17 for one of the 4-GHz channels. This points up the problems of using a best fit line to estimate tail probabilities. Within such limitations it appears that the simple aL^2 model for the hourly and daily variations of multipath fade time is adequate.

7.8 *Empirical Probability Distribution of the Median of the Fade Depth Distribution for a Minute in a Fading Hour*

In preceding sections, the multipath fading data have been examined on a daily basis (Sections 7.2 and 7.6) and an hourly basis (Sections 7.3, 7.4, 7.5, and 7.7). Finer scale variations also are of interest. The sampling rate for a single radio channel varies from 0.2 second to 30 seconds depending on the amount of activity. This suggests that the smallest consecutive time interval that can be used in the construction of fade depth distributions is one minute. The measurement technique guarantees that if the 30-second rate is being used then the difference between any two 30-second samples is less than 2 dB.

The previous section (7.7) gave an estimate of the probability distribution of the hourly median fade depth of a fading hour. It is logical then to consider the median of the fade depth distribution for each minute within a clock hour. One channel in each of the three bands, 4, 6, and 11 GHz, was selected for study during five hours with multipath activity. The hourly medians in dB for each combination are given in Table VII. Four of the hours selected were drawn from among the ten having the most fading, with one lesser fading hour (day 10, 5–6 A.M.) included for comparison.

The data analysis for the five hours proceeds as follows:

(*i*) Construct the experimental fade depth distribution for each minute within the hour and for the entire hour.

(*ii*) Estimate the 50-percent dB point from the fade depth distribution for: (a) each minute within the hour: m_i dB, $1 \leqq i \leqq 60$; (b) the entire hour: h dB.

(*iii*) Calculate the difference in minute and hour medians:

$$d_i = h - m_i \text{ dB}. \tag{25}$$

(*iv*) Rank order the d_i values from largest to smallest (i is then

TABLE VII—MEDIAN VALUES OF THE HOURLY FADE DEPTH DISTRIBUTION

Day	Hour	4 GHz	6 GHz	11 GHz
10	2–3 A.M	①* −20.5 dB	② −23.5 dB	① −27.5 dB
	3–4 A.M.	③ −17.4 dB	④ −21.0 dB	② −22.7 dB
	5–6 A.M.	㉕ −11.5 dB	⑰ −13.0 dB	⑳ −14.2 dB
28	0–1 A.M.	⑦ −16.4 dB	⑩ −16.2 dB	⑦ −17.4 dB
43	5–6 A.M.	⑥ −17.5 dB	① −22.8 dB	③ −21.0 dB

* The circled numbers give the hourly rank order position of the fade time at or below level 3 (−31.0 dB) in the hour.

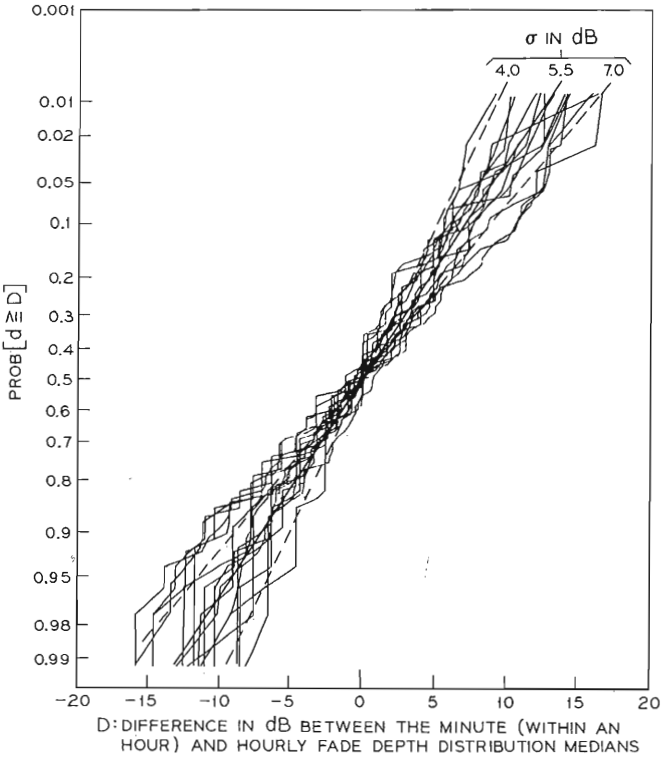

Fig. 23—Cumulative empirical probability distribution for the difference between the minute and hourly fade depth distribution medians. Data samples of five hours for 4, 6, and 11 GHz.

redefined as the rank order index with $i = 1$ for the worst 50-percent minute median fade value as normalized to the hourly median).

(v) Construct the cumulative empirical probability distribution for d, that is,

$$\Pr [d \geqq d_i] \cong \frac{i - 0.5}{60}. \tag{26}$$

The c.e.p.d. for d is plotted on Fig. 23 for all five hours and the three radio channels. This single plot suffices because there is no consistent difference between the different hours for a particular channel or between the different channels in a particular hour. As expected, the 50-percent point falls at the 0-dB difference point (within ± 1 dB). The entire set of data appears to be normal with a mean of 0 dB and a standard deviation of 5.5 $\pm$ 1.5 dB. It can be seen that, for a multipath fading hour, the minute medians vary considerably as compared to the hourly median. This is not surprising since the average duration of a multipath fade varies from 4 seconds at a -40-dB fade depth to 40 seconds at a -20-dB fade depth.[4]

To recapitulate, the hourly median can be estimated from Fig. 22 using equation (24) and the difference in the hourly and minute median calculated using a normal distribution with a mean of 0 dB and σ = 5.5 dB.

VIII. AMPLITUDE STATISTICS FOR ENTIRE TEST PERIOD

8.1 *Introduction*

The effects of multipath propagation are most important in the deep fade region, because the received signal can be rendered unusable. The signal statistics for shallow fade depths also are of interest if only because the signal amplitude resides in this range for the vast majority of time. At West Unity an elapsed time of 5.26×10^6 seconds (T_o) was the total data base; of this total 0.78×10^6 seconds (T_A) contained all the deep multipath fading and was subjected to detailed analysis.[1,2,4] In this section, statistics for the remaining 4.48×10^6 seconds (T_B) will be presented for two 4-GHz and two 6-GHz channels. The data for the 11-GHz channel was not included in this analysis because of the difficulty of separating out the effects of rain attenuation.

8.2 *Fade Depth Distribution*

The fade depth distributions for 4 and 6 GHz are given on Figs. 24 and 25, respectively, for the three time bases T_A, T_B, and $T_o = T_A + T_B$.

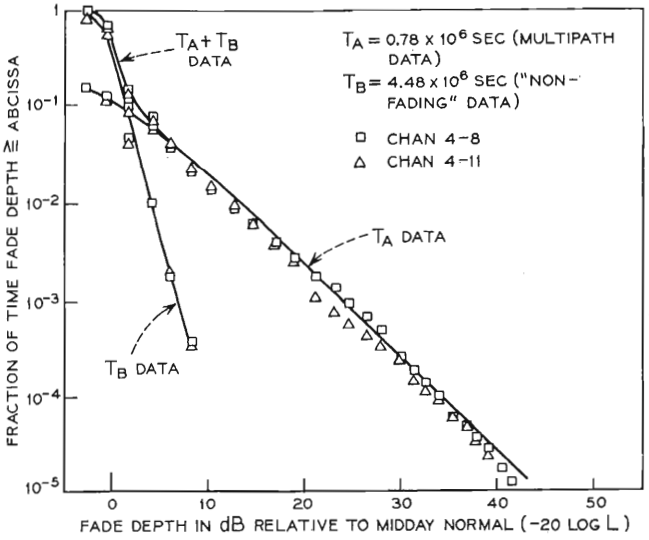

Fig. 24—4-GHz fade depth distribution for the entire test period, 1966 West Unity.

The lines on the figures are smoothed through the data, with the deep fade equations $0.25L^2$ and $0.53L^2$ (as given in Table II) used below -20 dB for 4 and 6 GHz respectively. As expected, the T_B data dominates the total distribution above the 10-percent point.

It should not be inferred from these results that there was zero probability of upfades above $+3$ dB. The equipment was designed to give this value whenever the signal level was in excess thereof.

The data for the fade depths less than 20 dB have been replotted on Figs. 26 and 27 on a normal probability scale where each set of data has been normalized to its own time base, e.g., the data for the multipath period are expressed as a fraction of 0.78×10^6 seconds (T_A). The data are given for only one of the channels in each band since the two channels have almost identical statistics in this fade depth range (see Figs. 24 and 25).

The plots show that neither the data for the total measurement period of 5.26×10^6 seconds ($T_A + T_B$) nor for the "nonfading" period of 4.48×10^6 seconds (T_B) are lognormal. During normal daytime periods of transmission on a single hop when the atmosphere is well mixed the envelope voltage scintillates and has a lognormal distribution with a standard deviation less than 1 dB. The T_B data is drawn from

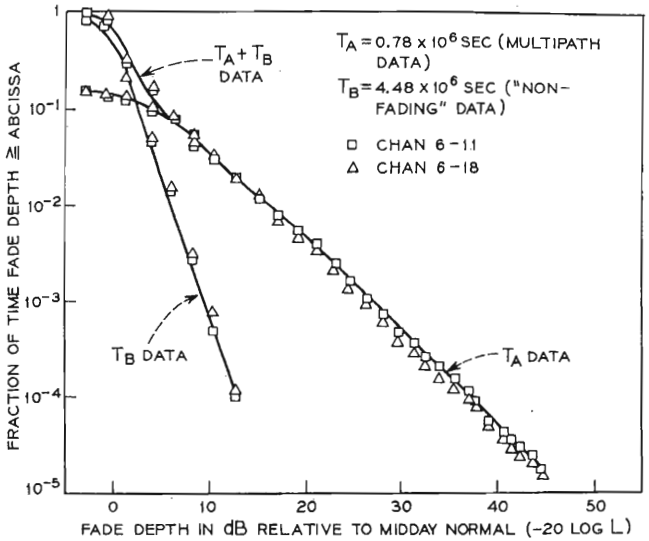

Fig. 25—6-GHz fade depth distribution for the entire test period, 1966 West Unity.

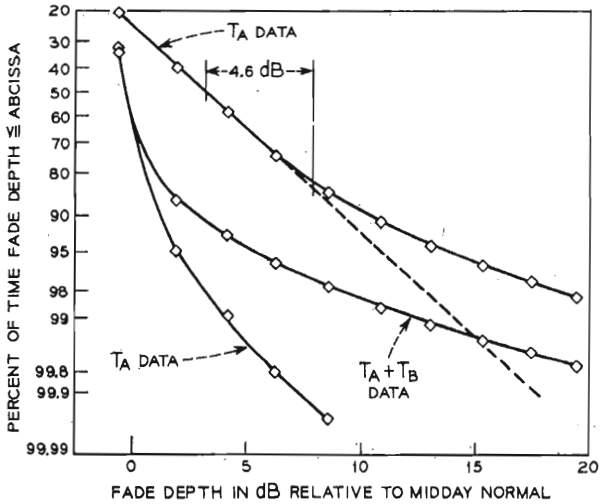

Fig. 26—4-GHz fade depth distribution, 1966 West Unity, probabilities for measurement intervals T_A (0.78×10^6 seconds), T_B (4.48×10^6 seconds), and $T_A + T_B$ (5.26×10^6 seconds).

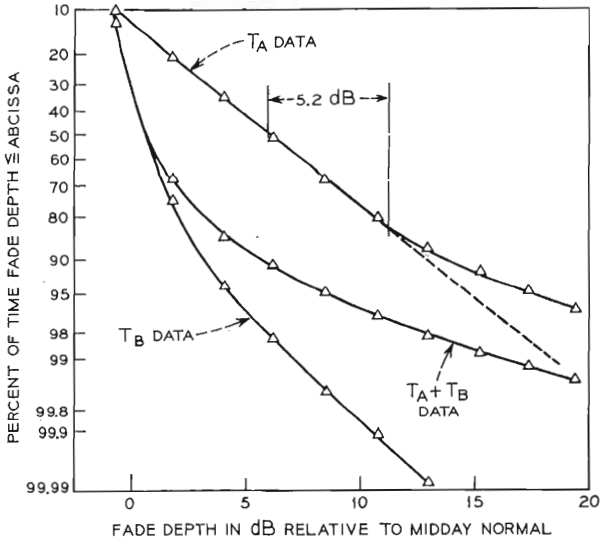

Fig. 27—6-GHz fade depth distribution, 1966 West Unity, probabilities for measurement intervals T_A (0.78×10^6 seconds), T_B (4.48×10^6 seconds), and $T_A + T_B$ (5.26×10^6 seconds).

a mixture of such periods and others with mild fading. This mixture, coupled with the approximately 2-dB quantizing intervals, makes it difficult to draw definitive conclusions from either the T_B or the $(T_B + T_A)$ data in the central part of the distribution.

The T_A data are approximately lognormal over the central 80 percent of the distribution, with the characteristics given in Table VIII. As can be seen from Figs. 26 and 27, the lognormal characteristic is useless for predicting the deep fade behavior. This seems to be a common finding; an observable which can be modeled as having multiplicative components is usually lognormal near its median. However, a more sophisticated model is needed for calculation of the tails of the distribution.[7]

TABLE VIII—CHARACTERISTICS OF SHALLOW FADES DURING PERIODS INCLUSIVE OF ALL DEEP MULTIPATH FADES

Characteristic	4 GHz	6 GHz
50% point	3.1 dB	6.0 dB
σ	4.6 dB	5.2 dB

8.3 *Number of Fades and Average Fade Durations*

Data on the number of fades and the average fade duration were also obtained for a 4-GHz and a 6-GHz radio channel, as shown on Figs. 28a–b and 29a–b respectively. The number of fades occurring during the deep fade total time (T_A) first increases and then decreases as the fade depth increases below 0 dB. The line through the deep fade region, $3670L$ for 4 GHz on Fig. 28a and $6410L$ for 6 GHz on Fig. 29a, are the least squares fitted lines to the data for all the channels in the separate bands.[4] The data for the balance of the measurement time (T_B) varies more rapidly as a function of fade depth, i.e., approximately a factor of 100 from 0 to −10 dB. Of course, the T_B data has many more fades at 0 dB fade than the T_A data. Note that the deep fade fitted line would overestimate the number of fades by a factor of 2 at a −10-dB fade depth but would be quite adequate for prediction at 0 dB fade depth.

The average fade duration at any fade depth is obtained from the ratio of the total time at or below the fade depth to the number of fades of this depth. Values for this variable have been obtained from the data for each of the three time bases—T_A, T_B, and $T_A + T_B$—as shown on Figs. 28b and 29b for 4 and 6 GHz respectively. The lines $408L$ (4 GHz) and $490L$ (6 GHz) have been obtained for the deep fade

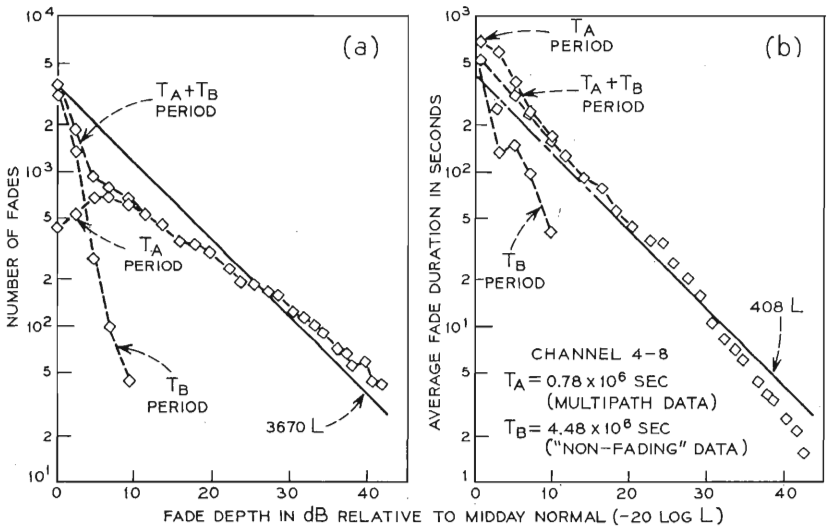

Fig. 28a—4-GHz number of fades for the entire test period.
Fig. 28b—4-GHz average fade duration for the entire test period.

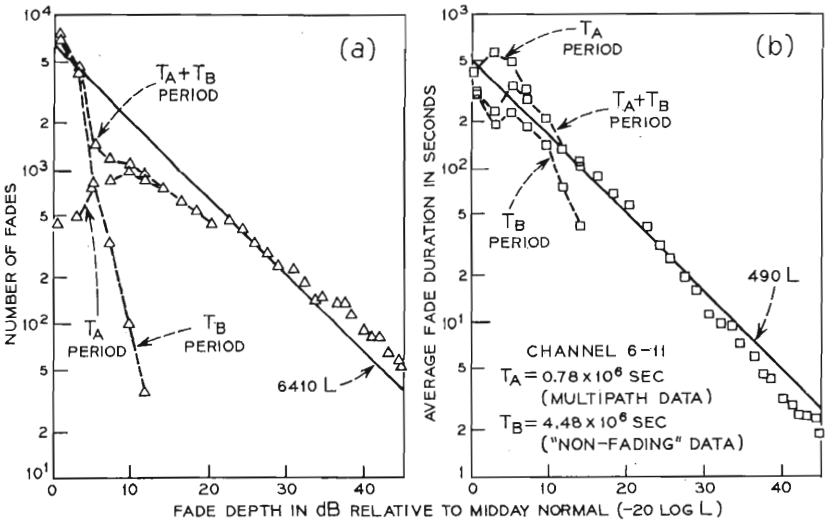

Fig. 29a—6-GHz number of fades for the entire test period.
Fig. 29b—6-GHz average fade duration for the entire test period.

data. However, these deep fade lines, extended to 0 dB, are a good representation of the data for the entire dB range. This is further evidence in support of Lin's finding that the average fade duration is less sensitive to the fading conditions than is either the number of fades or the fade depth distribution.

IX. ACKNOWLEDGMENTS

The author is indebted to many of his colleagues. The experimental data was obtained by MIDAS which was the creation of G. A. Zimmerman. The computer data processing capability was provided by C. H. Menzel. The data tabulation and plots were done by Miss E. J. Emer and Miss P. L. Russell. The interest and support of E. E. Muller and K. Bullington were invaluable.

REFERENCES

1. Vigants, A., "The Number of Fades in Space-Diversity Reception," B.S.T.J., *49*, No. 7 (September 1970), pp. 1513–1530.
2. Barnett, W. T., "Microwave Line-of-Sight Propagation With and Without Frequency Diversity," B.S.T.J., *49*, No. 8 (October 1970), pp. 1827–1871.
3. Chen, W. Y. S., "Estimated Outage in Long-Haul Radio Relay Systems with Protection Switching," B.S.T.J., *50*, No. 4 (April 1971), pp. 1455–1485.
4. Vigants, A., "Number and Duration of Fades at 6 and 4 GHz," B.S.T.J., *50*, No. 3 (March 1971), pp. 815–841.

5. Beckmann, P., and Spizzichino, A., *The Scattering of Electromagnetic Waves from Rough Surfaces*, New York: Pergamon Press, 1963, pp. 355–367.
6. Ruthroff, C. L., "Multiple-Path Fading on Line-of-Sight Microwave Radio Systems as a Function of Path Length and Frequency," B.S.T.J., *50*, No. 7 (September 1971), pp. 2375–2398.
7. Lin, S. H., "Statistical Behavior of a Fading Signal," B.S.T.J., *50*, No. 10 (December 1971), pp. 3211–3270.
8. Pearson, K. W., "Method for the Prediction of the Fading Performance of a Multisection Microwave Link," Proc. IEE, *112*, No. 7 (July 1965), pp. 1291–1300.
9. Yonezawa, S., and Tanaka, N., *Microwave Communication*, Tokyo: Maruzen Co., Ltd., 1965, pp. 25–60.
10. Wilk, M. B., and Gnanadesikan, R., "Probability Plotting Methods for the Analysis of Data," Biometrika, *55*, No. 1 (1968), pp. 1–17.